




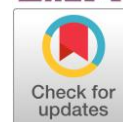
# Chitosan-based polyelectrolyte complex in combination with allotropic forms of carbon as a basis for thin-film organic electronics

Rufina Zilberg<sup>a\*</sup> , Renat Salikhov<sup>b</sup> , Ilnur Mullagaliev<sup>b</sup>, Yulia Teres<sup>a</sup>, Elena Bulysheva<sup>a</sup>, Timur Salikhov<sup>b</sup>, Anastasia Ostaltsova<sup>b</sup>, Ivan Vakulin<sup>a</sup> 

**a:** Institute of Chemistry and Protection in Emergency Situations, Ufa University of Science and Technology, Ufa 450076, Russia

**b:** Physical and Technical Institute, Ufa University of Science and Technology, Ufa 450076, Russia

\* Corresponding author: [ZilbergRA@yandex.ru](mailto:ZilbergRA@yandex.ru)



This paper belongs to a Regular Issue.

## Abstract

Using atomic force microscopy, scanning electron microscopy, cyclic voltammetry and electrochemical impedance spectroscopy, the morphology and mobility of charge carriers in composite films with a thickness of no more than 500 nm obtained on the basis of a polyelectrolyte complex of chitosan and chitosan succinamide with addition of particles of carbon materials were studied and estimated. The following carbon materials were used: single-walled carbon nanotubes, graphene oxide, and carbon-containing sorbents with different specific surfaces (Carboblack C and Carbopack). Moreover, the studied materials in the form of films were used as a transport layer in the structure of field-effect transistors. The output and transfer characteristics of the transistors obtained were measured. According to the measurement results, the mobility of charge carriers,  $\mu$ , ranges from 0.341 to 1.123 cm<sup>2</sup> V<sup>-1</sup>·s<sup>-1</sup>, depending on the type of carbon material added. The best result was demonstrated by films based on a composite containing simultaneously single-walled carbon nanotubes and graphene oxide ( $\mu = 10.972$  cm<sup>2</sup> V<sup>-1</sup>·s<sup>-1</sup>).

## Key findings

- Samples of a new polymer composite material based on a PEC doped with various allotropic forms of carbon were prepared.
- Based on the films studied, field-effect transistors were created and their output and transfer characteristics were measured.
- If a combination of both GO and SWCNT is incorporated into the nanocomposite, the mobility of carriers increases sharply.

## Keywords

thin films  
polyelectrolyte complex of chitosan and chitosan succinate  
oxide graphene  
carboblack C  
carbopack  
SWCNT  
voltammetry  
field-effect transistor

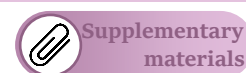
Received: 30.05.24

Revised: 11.06.24

Accepted: 19.06.24

Available online: 28.06.24

© 2024, the Authors. This article is published in open access under the terms and conditions of the Creative Commons Attribution (CC BY) license (<http://creativecommons.org/licenses/by/4.0/>).



## 1. Introduction

Flexible conductive polymers are among the most important materials for creating new-generation small-sized, energy-efficient wearable electronic devices. In addition to the basic requirements for the components of such devices, for example, charge mobility, gate resistance, permissible current, opening voltage, resistivity and others, parameters such as elasticity, flexibility and biocompatibility play an important role [1]. In many cases these requirements are mutually exclusive, and it seems to be a non-trivial task to

obtain a material with all the noted properties at the proper levels at the same time.

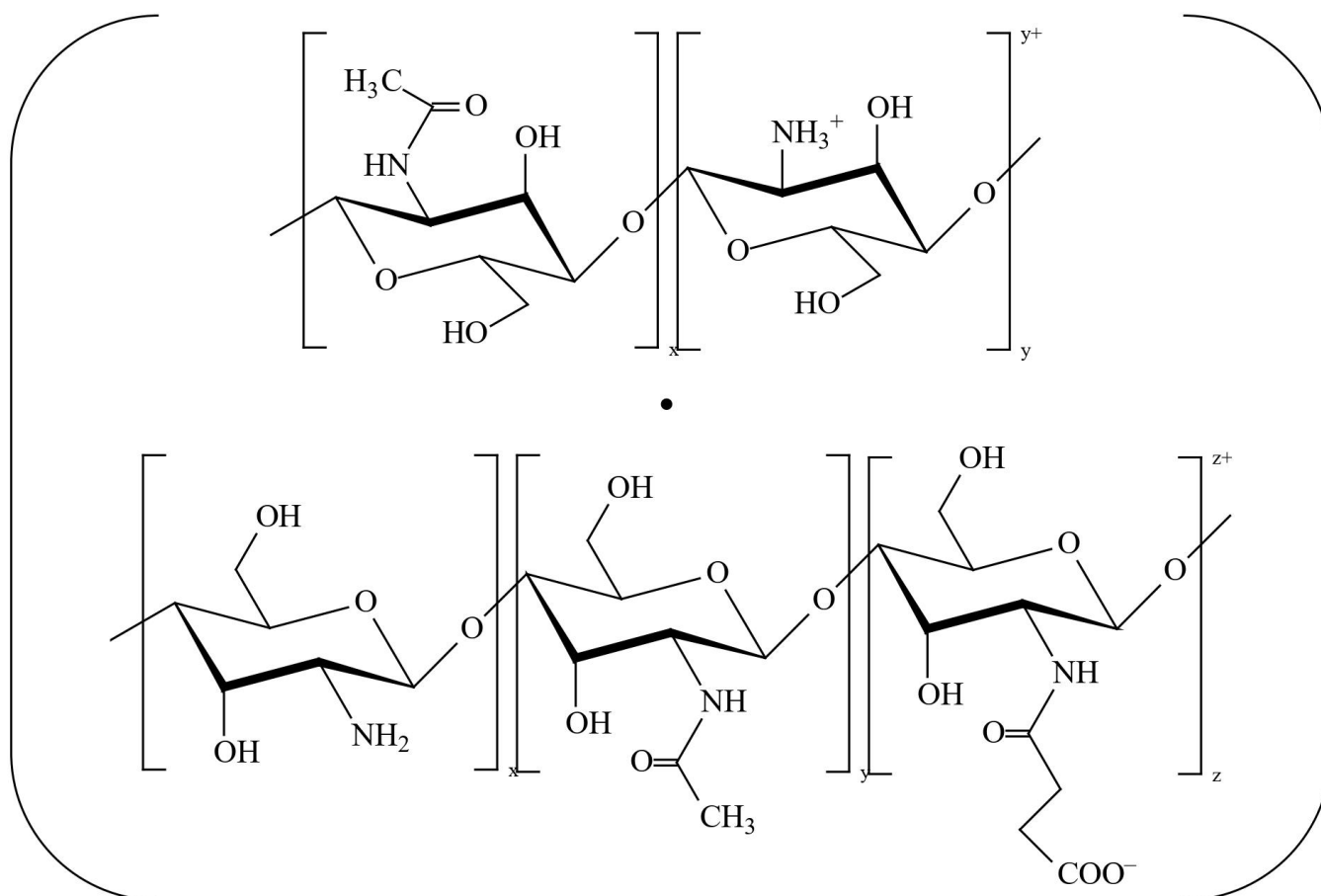
One of the drawbacks of conductive polymers is that they have low conductivity in thin films, and increasing the thickness to increase conductivity leads to a deterioration of the physical and mechanical properties, up to the loss of the required flexibility. One of the successful strategies to overcome the noted shortcomings in the creation of materials for flexible wearable devices is to use composites [2]. With this approach, it is possible to increase the conductivity or provide semiconductor properties by introducing

nanoparticles of substances with the desired properties into the matrix of a conductive polymer.

Carbon nanostructures of fullerenes [3–5], graphenes [3, 6], and carbon nanotubes [3, 7–11] seem to be very promising components of composite materials [11]. It is known that incorporation of carbon nanostructures into a polymer matrix, even in small quantities, increases the wear resistance of the material, its static and dynamic strength, while the spatial mesh of nanoparticles formed in the polymer matrix significantly increases the conductivity of the composite. Carbon nanotube transistors have been developed that surpass conventional silicon transistors in terms of charge mobility [12]. An equally important result of the dispersing carbon nanoparticles with various allotropic forms in a polymer matrix (multilayer (MWCNT) and single-layer carbon nanotubes (SWCNT), graphene, fullerenes, nanofibers) is that a variety of electrochemical sensors [3, 13–21], including enantiosensitive ones [22–25], as well as field-effect transistors [26–29] were created.

Equally important is the choice of the polymer matrix base, since not every conductive polymer has the required biocompatibility. In this regard, polyelectrolyte complexes (PEC) based on natural polymers are of great interest, for example, those based on a polycation such as chitosan hydrochloride and a polyanion such as chitosan succinate sodium salt (Figure 1) [30–32]. The thin films prepared from such complexes have a unique combination of

physicochemical [33] and biological properties [34–39], e.g., biocompatibility and antimicrobial activity, which is essential in creating sensors to be implanted in living organisms. It is important to note that PEC based on chitosan-chitosan succinimide do not require a complex production technology [31] and are spontaneously formed by mixing oppositely charged solutions of polyelectrolytes in water without the use of organic solvents, chemical crosslinking or surfactants [40]. The PEC indicated above has been successfully used as a modifier in the creation of enantioselective electrochemical sensors [25, 41–42] and multisensory systems [43]. Examples of the incorporation of molecules and nanoparticles into a film based on polyelectrolyte complexes are known: nanoparticles of platinum [44], gold [45], ferrocenium ions [46], carbon-containing sorbents (Carboblack C) [25], graphene oxide and carbon nanotubes [47–48]. It has been shown that doping of PEC with carbon nanomaterials provides high electrical conductivity, chemical inertness, a large ratio of the edge and base planes, a large area of the effective sensor surface due to a high degree of roughness. Moreover, the possibility of nanomaterial surface functionalization increases the sensitivity of response to an analyte at low concentrations or in a complex matrix and provides lower detection limits and fast electron transfer compared to pure PEC, i.e., improves the analytical characteristics in the determination of the target analytes [15].



**Figure 1** The structure of PEC based on chitosan (polycation) and chitosan succinate (polyanion).

This work deals with the creation and study of new composite thin-film structures based on a chitosan-chitosan succinamide polyelectrolyte complex, where the following carbon nanomaterials were used as the fillers: single-walled carbon nanotubes, graphene oxide and carbon-containing sorbents with various specific surfaces (Carboblack C and Carbopack). The study of the physicochemical characteristics of the initial composite and nanocomposite material is a prerequisite for the creation of efficient sensor platforms with enhanced electroanalytical parameters and field-effect transistors with good output and transfer characteristics.

## 2. Materials and Methods

### 2.1. Materials and reagents

All the chemicals and solvents used in the electrochemical studies were of analytical reagent grade and were used as received without further purification. Ultrapure deionized water was used in all the experiments ( $0.11 \mu\text{S}/\text{cm}$ ).

The PEC of polysaccharide nature was prepared on the basis of a polycation (chitosan hydrochloride) and a polyanion (chitosan succinamide sodium salt) (JSC "Bioprogress", Russia). The chitosan succinate sodium salt (molecular weight 200 kDa) was obtained from chitosan with the degree of deacetylation of 82% and the degree of modification by amino groups of 75%. Chitosan hydrochloride was taken in the form of a film obtained from a chitosan solution in hydrochloric acid, which was prepared by dissolving 0.25 g of chitosan (molecular weight 30 kDa) with a deacetylation degree of 75% in 50 ml of 1% HCl. The films were dried in air followed by vacuum drying to a constant mass. Aqueous dispersions of PEC were obtained at a temperature of 25 °C by dropwise addition of an aqueous solution of chitosan hydrochloride (0.005%) to an aqueous solutions of chitosan succinate (0.005%) with vigorous stirring (500 rpm), with a 2-minute interval between the addition of portions. As new portions of the chitosan hydrochloride solution were added to the resulting solution, phase separation occurred (stable opalescence of the entire system appeared). The region where dispersions of PEC particles of these polysaccharides exist is limited by a molar ratio of 0.1, above which precipitation of the complex is observed during the mixing of the components [27–28].

Nanocomposites and composites were prepared by dissolving of the following components in 1 ml PEC: 0.001, 0.002 and 0.003 g SWCNT (diameter 0.7–1.1 nm) (Sigma-Aldrich, USA), graphene oxide GO (powder: 15–20 sheets, 4–10% edge-oxidized) (Sigma-Aldrich, USA), Carboblack C (specific surface area  $10 \text{ m}^2/\text{g}$ , particle size 60–80 mesh (0.18–0.25 mm) (Restek, USA), and Carbopack (specific surface area  $100 \text{ m}^2/\text{g}$ , particle size 60–80 mesh (0.18–0.25 mm) (Sigma-Aldrich, USA), followed by exposure for 60 min in an ultrasonic bath (operating frequency 35 kHz).

A solution of the equimolar redox probe  $[\text{Fe}(\text{CN})_6]^{4-/3-}$  (5.0 mM) was prepared using 0.1 M KCl solution as the background electrolyte.

### 2.2. Modification of the GCE

10  $\mu\text{l}$  of the prepared solution of PEC, PEC-CarboblackC, PEC-Carbopack, PEC-GO and PEC-SWCNT were withdrawn with an automatic pipette and applied to the surface of pre-polished GCE (drop-casting); then the electrode was dried for 6 min at 80 °C under an infrared lamp and cooled at room temperature for 3 min. Before each measurement, the GCE surface was polished for 1 min using a deagglomerated suspension based on 0.3  $\mu\text{m}$  of  $\text{Al}_2\text{O}_3$  and a Spec-Cloth Adhesive black disk polishing material (Allied High Tech Products Inc., USA), followed by repeated washing of the electrode with deionized water and air-drying at room temperature.

### 2.3. Equipment and devices

Electrochemical measurements, including cyclic voltammetry (CV) and electrochemical impedance spectroscopy (EIS), were carried out using an AUTOLAB PGSTAT 204 potentiostat/galvanostat with a FRA 32M module (Metrohm Autolab Ins., Netherlands) with Nova software in a three-electrode cell comprising an unmodified or modified glass-carbon electrode (Metrohm) 2 mm in diameter as the working electrode, a silver-silver chloride reference electrode with saturated KCl, and platinum wire as the auxiliary electrode. All measurements were carried out at room temperature ( $22 \pm 0.5$  °C). An ultrasonic bath (Elmsonic One, Germany) was used to prepare PEC composites with carbon particles.

To study the surface morphology of thin composite films and PEC films, two microscopes were used: a Nanoeducator II NT-MDT atomic force microscope and a TESCAN MIRA LMS scanning electron microscope (SEM) with TESCAN Essence software.

### 2.4. Experimental technique

The voltammetric and electrochemical impedance characteristics of GCE, GCE/PEC, GCE/PEC-CarboblackC, GCE/PEC-Carbopack, GCE/PEC-GO, and GCE/PEC-SWCNT electrodes were studied in a standard 5 mM  $[\text{Fe}(\text{CN})_6]^{4-/3-}$  solution prepared using 0.1 M KCl. The  $[\text{Fe}(\text{CN})_6]^{4-/3-}$  redox probe solution with a volume of 20 ml was placed into an electrochemical cell. A CV was recorded in the potential range from 0.6 to 1.0 V at a scan rate of 0.1 V/s. Impedance spectra were recorded in an AC frequency range from 50 kHz to 0.1 Hz, with an amplitude of 5 mV. The data array for each sample consisted of five parallel measurements, which was enough to obtain reproducible results. The composites were stored for 5 days in the refrigerator at a temperature of 4 °C.

The samples of field-effect transistors (Figure 2) were created from composites based on PEC: PEC-CarboblackC, PEC-Carbopack, PEC-GO and PEC-SWCNT. The samples of field-effect transistors were made on a glass substrate containing layers of ITO (gate). Before creating the dielectric films, the substrates were annealed in a furnace at 350 °C. Dielectric, 300 nm thick  $\text{AlO}_x$  films were created by

centrifugation from a solution at 2000 rpm for 30 s followed by annealing in an oven for 1 hour at 350 °C. Two aluminum electrodes, a drain and a source 500 nm in thickness, were applied on top of the gate dielectric. A layer of a semiconductor material of the four types listed above was deposited in the gap area by centrifugation. The gap between the drain and source contacts was 50 μm, and the gap length was 2 mm. The following devices were used to measure the voltametric characteristics: Mastech HY3005D-2 power supply and Tektronix DMM-4020 multimeter as an ammeter.

### 3. Result and Discussion

#### 3.1. Choosing the optimal compositions of the composites

In choosing the optimal compositions of composites based on PEC and carbon nanoparticles, the optimality criteria included the values of the maximum oxidation peak currents of the standard redox probe of potassium hexacyanoferrate (II /III). The effect of the concentration of nanoparticles: Carboblack, Carbopack, GO, SWCNT in PEC on the voltametric characteristics of an equimolar mixture of potassium hexacyanoferrate (II/III) was estimated. It was found that the potentials of oxidation and reduction did not change, while the variation of the oxidation currents was statistically significant (Figure 3). With an increase in the concentration of CarboblackC and Carbopack nanoparticles from 1 to 2 mg/ml, an increase in oxidation currents was observed, while a further increase in the content of CarboblackC and Carbopack nanoparticles led to an increase in the relative standard deviation, i.e. to a decrease in the reproducibility of measurements. It was found that with an increase in the content of GO and SWCNT nanoparticles in the range from 1 to 3 mg/ml, the oxidation currents  $[\text{Fe}(\text{CN})_6]^{4-}$  increased (Figure 3). It can be assumed that this effect is associated with an increase in the effective surface area of the sensor and facilitation of electron transfer to the electrode surface due to addition of carbon nanoparticles to the PEC. However, a further increase in the content of GO and SWCNT led to an increase in the relative standard deviation. Thus, composites obtained using the concentration of CarboblackC and Carbopack nanoparticles of 2 mg in 1 ml of PEC, or 3 mg in 1 ml of PEC in the case of GO and SWCNT, were selected for further studies.

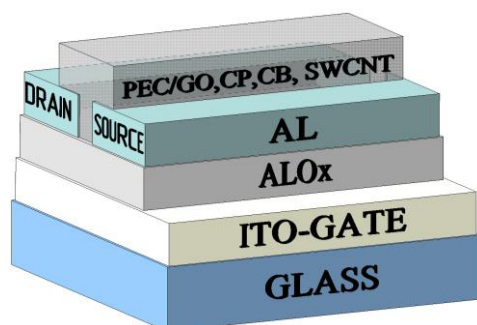


Figure 2 Structure of the experimental field-effect transistor.

#### 3.2. Electrochemical behavior of various modified electrodes

The CVs of various modified electrodes in 0.1 M KCl containing 5 mM  $[\text{Fe}(\text{CN})_6]^{4-/3-}$  are shown in Figure 4a. A pair of well-defined redox peaks due to the conversion between  $[\text{Fe}(\text{CN})_6]^{4-}$  and  $[\text{Fe}(\text{CN})_6]^{3-}$  appears on all the electrodes tested. Compared to the unmodified GCE, the electrochemical signal clearly increased on all modified GCE, and the peak redox currents increased, which indicates that the modified electrodes have a larger electroactive surface area.

The electrochemical active surface areas on GCE and modified GCEs were determined from the CVs of 5 mM  $\text{K}_4[\text{Fe}(\text{CN})_6]$  in 0.1 M KCl solution. According to the Randles-Shevchik Equation 1 [44]:

$$I_p = (2.69 \cdot 10^5) n^{3/2} A D^{1/2} \nu^{1/2} C \quad (1)$$

where  $I_p$  (A) represents the peak current on the anode,  $n$  is the number of electrons participating in the redox reaction,  $A$  ( $\text{cm}^2$ ) is the area of a modified electrode,  $D$  ( $\text{cm}^2 \text{s}^{-1}$ ) represents the diffusion coefficient,  $\nu$  ( $\text{Vs}^{-1}$ ) is the scan rate, and  $C$  ( $\text{mol mL}^{-1}$ ) is the concentration of the oxidized form. For 5 mM  $[\text{Fe}(\text{CN})_6]^{4-/3-}$  with 0.1 M KCl,  $n = 1$  and  $D = 7.6 \cdot 10^{-6} \text{ cm}^2 \text{ s}^{-1}$ ,  $\nu = 0.1 \text{ Vs}^{-1}$ .

Figure 4a shows that a noticeable increase in the peak currents of the redox pair  $[\text{Fe}(\text{CN})_6]^{3-/4-}$  on cyclic voltammograms was observed after the addition of SWCNT and GO into the PEC film, which is associated with a decrease in the charge transfer resistance and indicates that SWCNT and GO dispersed in PEC are materials with good conductivity [13-14].

Electrochemical impedance spectroscopy (EIS) was used to characterize the electron transfer on the electrodes under consideration [45]. Figure 4b shows the corresponding Nyquist plots. The semicircle in the high frequency region corresponds to the limiting stage of charge transfer. The rectilinear section in the region of lower frequencies describes the diffusion component of charge transfer.

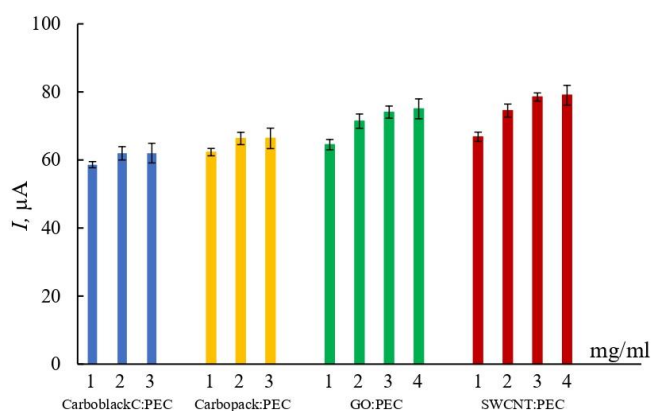


Figure 3 Effect of concentrations of carbon nanoparticles in the CarboblackC:PEC, Carbopack:PEC, GO:PEC, and SWCNT:PEC composites on the oxidation currents of 5.0 mM  $[\text{Fe}(\text{CN})_6]^{3-/4-}$  solution against the background of 0.1 M KCl according to cyclic voltammetry. The mean values and confidence intervals are given ( $n = 5$ ,  $P = 0.95$ ).



The diameter of the semicircle for modified electrodes is significantly smaller than that for GCE, which indicates an increase in the charge transfer rate. For quantitative interpretation of the EIS data, an equivalent Randles cell was used that consisted of the following components:  $R_s$  (solution resistance), which is the sum of the intrinsic resistance of the active material, the electrolyte solution resistance, and the contact resistance at the electrode/electrolyte interface;  $R_{et}$  (charge transfer resistance) that depends on the insulating features at the electrode/electrolyte interface;  $C_{dl}$  (constant phase element) that is the double layer capacitance;  $W$  (Warburg element) that is closely related to the electrochemical controlled diffusion process. The results obtained are presented in Table 1. As can be seen from the table data, for the modified electrodes, there is a significant decrease in the charge transfer resistance compared to the GCE (3.07 times for GCE/PEC, 5.94 times for GCE/PEC-CarboblackC, 8.31 times for GCE/PEC-Carbopack, 9.13 times for GCE/PEC-GO and 16.27 times for GCE/PEC-SWCNT), which confirms the increase in the charge transfer rate. Thus, the greatest efficiency of electronic transfer is characteristic of the electrode modified by PEC-SWCNT, which closely agrees with the CV data.

Hence, the composite films studied have a sufficient effective surface area and electron transfer rate. This makes it possible not only to use them to create electrochemical

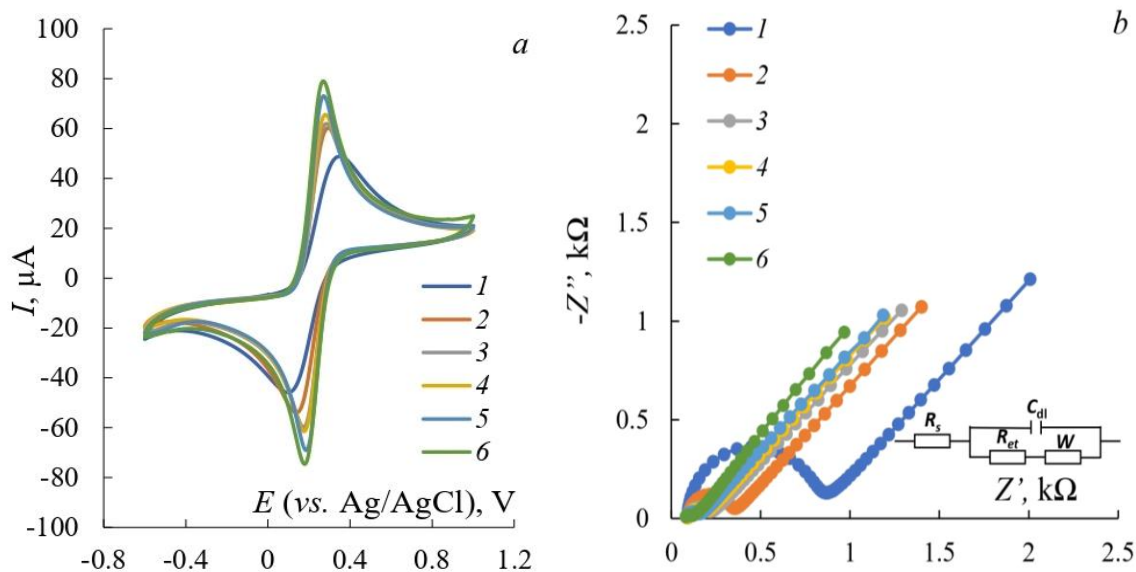
sensors, but also to consider them as a promising material for creating field-effect transistors.

### 3.3. Analysis of morphology structure

The morphology of the surface of the films was also studied. The AFM images (Figures 5 and 6) were obtained using Nanoeducator II.

Using the Gwyddion program, the root-mean-square roughness of the surface of the films over an area of  $20 \times 20 \mu\text{m}$  with an error of up to 10% was calculated and presented in the diagram (Figure 7). The roughness values thus obtained correlate with the effective surface area values given above.

Analysis of reflected secondary electrons (Oxford instruments Aztec EMF version 6.0 sp<sup>1</sup>) was used to study the distribution of chemical elements on the film surfaces. The SEM images (Figure 8) show the distribution of carbon (in yellow) over the surface of the film. The SEM images show changes in the morphology of films in the transition from pure PEC to its composites with SWCNT or GO. So, the surface of pure PEC is quite homogeneous, while on the PEC/SWCNT samples the nanotubes are represented as a fibrous structure with non-uniform density over the surface of the sample. The structures associated with GO are evenly distributed over the entire surface, but at the same time they form large "island" sections.



**Figure 4** Cyclic voltammograms (a) and Nyquist plots (b) for 5.0 mM solution of  $[\text{Fe}(\text{CN})_6]^{3-/4-}$  against the background of 0.1 M KCl on various electrodes: 1 - GCE, 2 - GCE/PEC, 3 - GCE/PEC-CarboblackC, 4 - GCE/PEC-Carbopack, 5 - GCE/PEC-GO, 6 - GCE/PEC-SWCNT. Insert: the Randles equivalent circuit used for data analysis.

**Table 1** Parameters of electrochemical impedance spectra and the effective surface area according to CV of GCE and modified GCE in 5.0 mM  $[\text{Fe}(\text{CN})_6]^{4-/3-}$  ( $n = 5$ ;  $P = 0.95$ ).

Sensor	A, mm <sup>2</sup>	$R_s$ , $\Omega$	$R_{et}$ , $\Omega$	$C_{dl}$ , $\mu\text{S}$	W, $\mu\text{S}$
GCE	7.93±0.06	89±4	768.0±0.2	1.02±0.03	782±5
GCE/PEC	10.33±0.06	87±3	250.1±4.1	1.53±0.07	846±11
GCE/PEC-CarboblackC	10.57±0.13	85±2	129.3±0.9	1.71±0.08	810±9
GCE/PEC-Carbopack	11.31±0.11	84±3	92.4±1.9	2.17±0.05	875±8
GCE/PEC-GO	12.63±0.19	78±3	84.1±1.7	2.27±0.03	857±5
GCE/PEC-SWCNT	13.39±0.18	73±2	47.2±2.5	3.45±0.09	1050±3

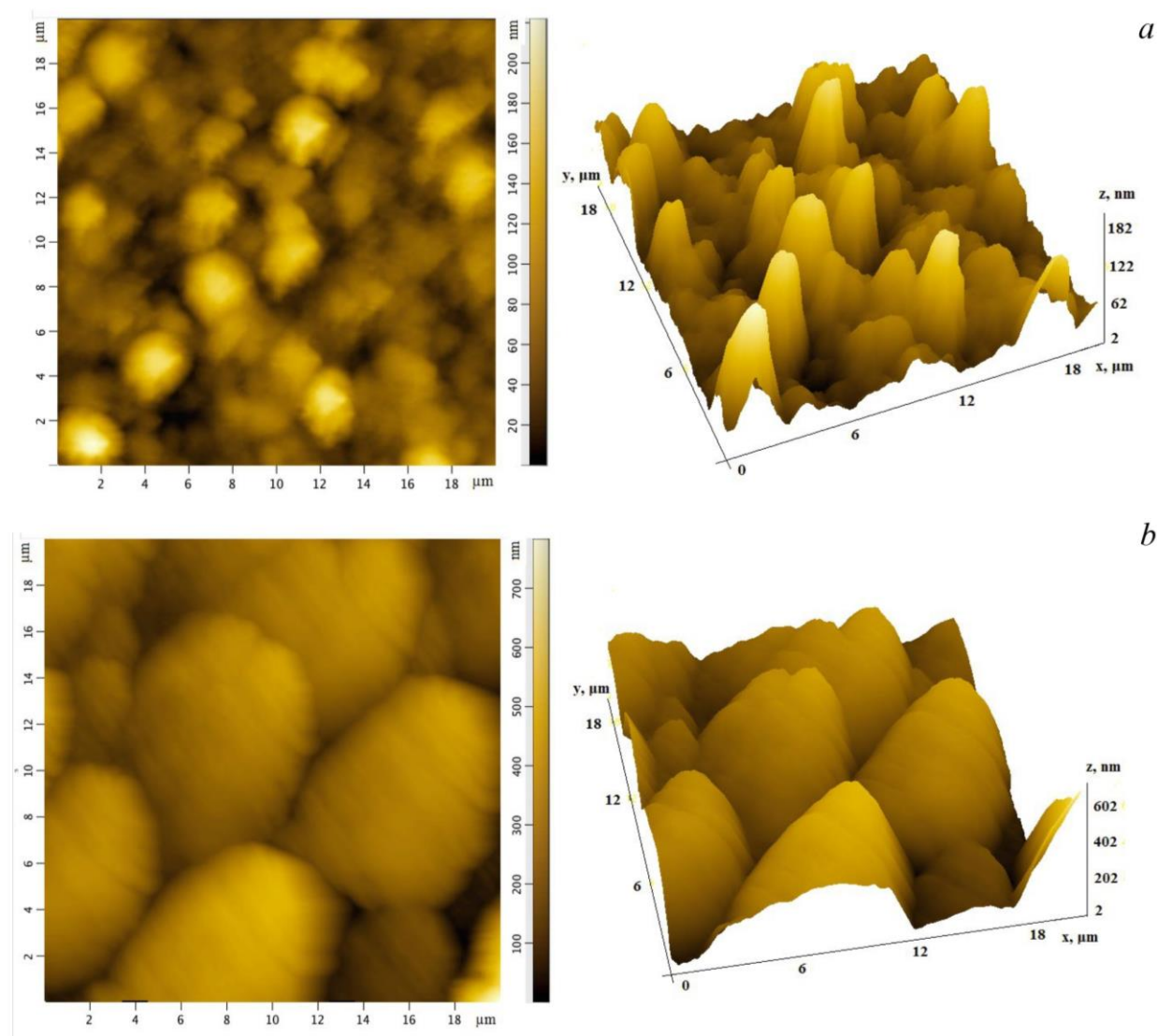


Figure 5 AFM images 20×20 μm: PEC (a), PEC-Carbopack (b).

### 3.4. Field-effect transistors

The current-voltage characteristics of the field-effect transistors (Figure 9) were recorded using the measurement scheme with a common source in open air at room temperature. The output current is controlled at a positive offset at the gate, which indicates the electronic type of conductivity in the composite films studied. In the case of polyelectrolyte complex films without additives, the lowest mobility of charge carriers is observed.

The mobility of charge carriers in the field-effect transistors obtained was determined using Equation 2:

$$\mu = \frac{I_{DS}}{\frac{W}{L} C (U_G - U_{th}) U_{DS}}, \quad (2)$$

where  $W$  is the channel width,  $L$  is the channel length,  $C$  is the capacitance per square area of the  $AlO_x$  gate dielectric (for a thickness of 500 nm,  $C = 7.1 \text{ nF/cm}^2$ ),  $U_G$  is the gate voltage,  $U_{DS}$  is the voltage between the drain and the source, and  $U_{th}$  is the threshold voltage. The threshold voltage  $U_{th}$  is found from the plots of the current root  $I_{DS}^{1/2}$  versus the voltage  $U_{DS}$  at  $U_G = \text{const}$ . The error of the calculated values was about 10%.

We compared found values of mobility of charge carriers for suggested chitosane based composite films with modern composite films taken from literature (Table S1)

Already the PEC itself shows good values of  $\mu$ , exceeding most of other composite films, because it has ionic nature in contrast to other polymers (PBTTT, P3HT, PAP, etc.) used in film composites. Only a few composite films based on sulfur-contained polymers, like pgBTTT [51], P(bgDPP-MeOT2) [52], p(gDPP-T2) [53], p(g2T-TT) [54], PProDOT-DPP [55], P3gCPDT-1gT2 [56] demonstrate better results (Table S1). It is interesting that PMMA/TiO<sub>2</sub>@PSAN-b-PAA-PDVB [57] composite film based on polymer without sulfur atoms in its monomer structure shows slightly better  $\mu$  value than the PEC film:  $0.500 \text{ cm}^2 \cdot \text{V}^{-1} \cdot \text{s}^{-1}$  vs  $0.314 \text{ cm}^2 \cdot \text{V}^{-1} \cdot \text{s}^{-1}$  (Table S1). Obviously, the close properties of the PMMA film are explained by the presence of carboxyl groups in the structure of PMMA and a similar ionic nature to PEC.

Introduction of carbon allotropic forms into the PEC film composition greatly increases the mobility of charge carriers, by up to 3.2 times (Table S1).

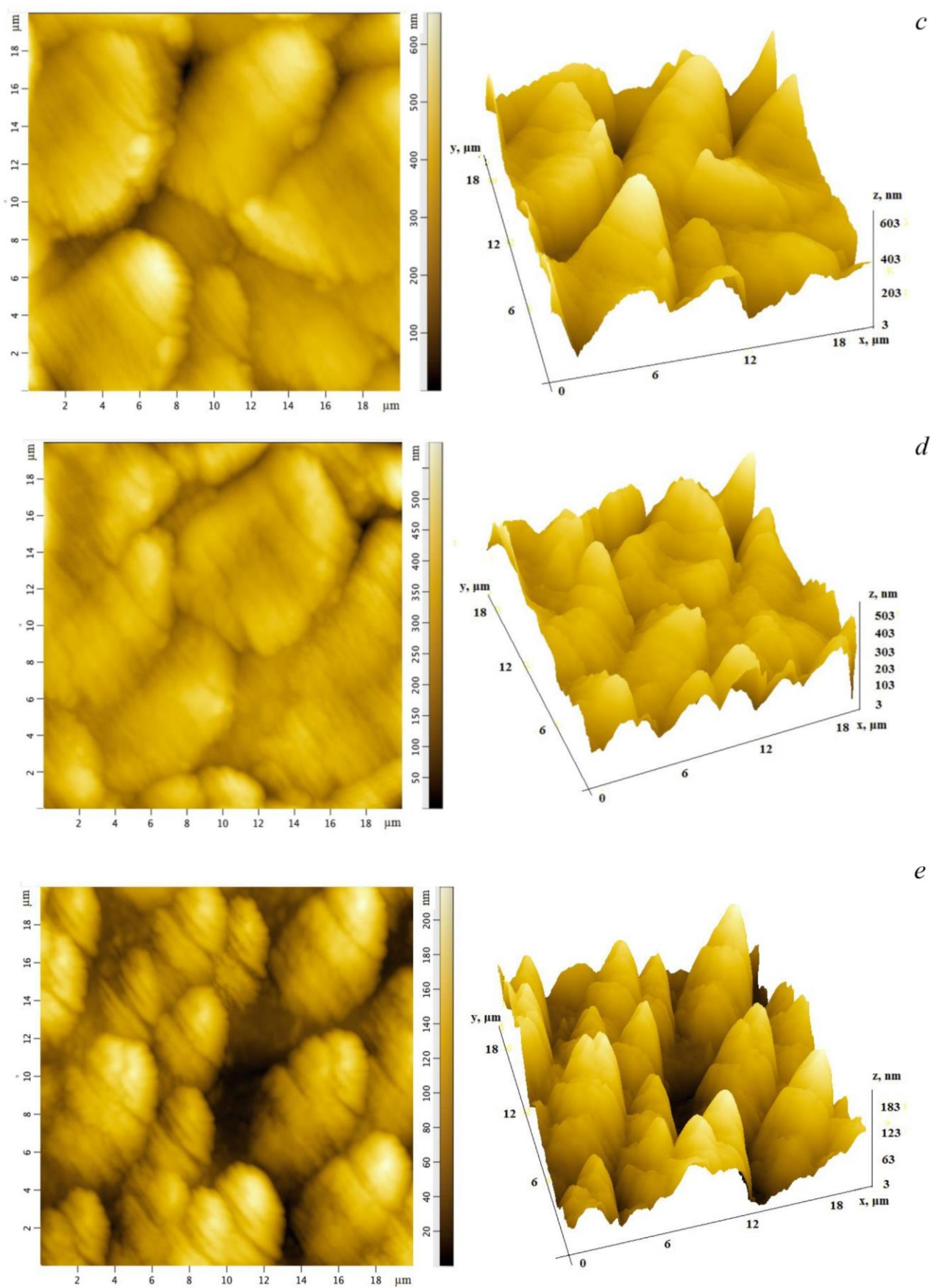
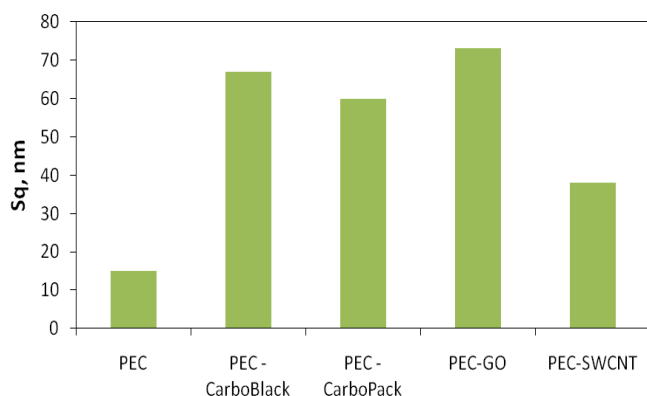


Figure 6 AFM images  $20 \times 20 \mu\text{m}$ : PEC-CarboBlackC (c), PEC-GO (d), PEC-SWCNT (e).





**Figure 7** Roughness values of the composite film samples.

The greatest impact is provided by the introduction of SWCNT; however, the more affordable and cheaper Carbopack increase the mobility by only 14% worse and are comparable in their influence with graphene oxide. The steepness of the current-voltage characteristics was determined at  $\Delta U$  from  $U = 4$  V to  $U = 10$  V (at  $U_{DS} = 6$  V). It was found that it was  $K = 0.86$  for a field-effect transistor based on PEC,  $K = 2.13$  for a transistor based on PEC-GO, and  $K = 2.66$  for PEC-SWCNT. A greater effect of the control voltage in transistors with a PEC-SWCNT transport layer was identified. Transistors with a transport layer made of nanocomposite materials based on PEC, SWCNT and GO were manufactured, and their characteristics were measured (Figure 10). The calculation of mobility resulted in values that were an order of magnitude higher ( $\mu = 10.97$   $\text{cm}^2 \cdot \text{V}^{-1} \cdot \text{s}^{-1}$ ) than in the PEC-GO and PEC-SWCNT transistors where the fillers were used separately. This can be explained by a synergistic effect that was also observed in a number of other studies [57].

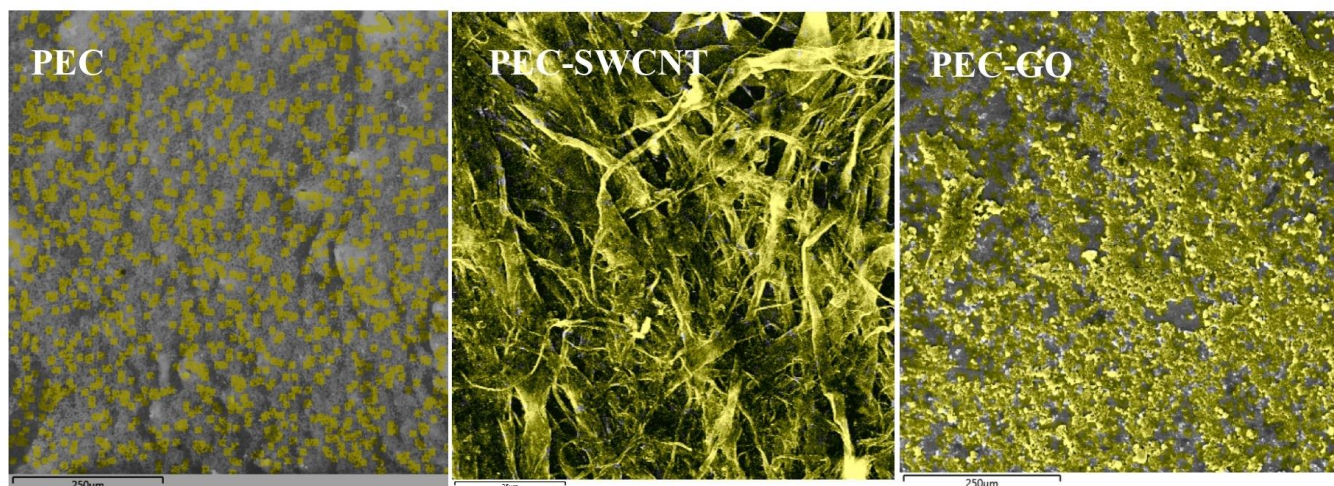
The charge carrier mobilities in materials similar to those presented in this article and on the basis of which thin-film field-effect transistors are made have the following values: for the composites with CNT – from 0.03 to

0.41  $\text{cm}^2 \cdot \text{V}^{-1} \cdot \text{s}^{-1}$  [58], for those with GO – from 0.06 to 0.86  $\text{cm}^2 \cdot \text{V}^{-1} \cdot \text{s}^{-1}$  [59] and for those with CarboBlackC – equal to 0.01  $\text{cm}^2 \cdot \text{V}^{-1} \cdot \text{s}^{-1}$  [60]. A large number of field-effect transistors based on polymer composites with carbon nanostructures have been created. The mobility of charge carriers in these transistors is in the range of 0.02–0.50  $\text{cm}^2 \cdot \text{V}^{-1} \cdot \text{s}^{-1}$ . The nanocomposite structures studied in this work have rather high mobility, especially the structure based on mixture combining GO+SWCNT [27].

## 4. Conclusions

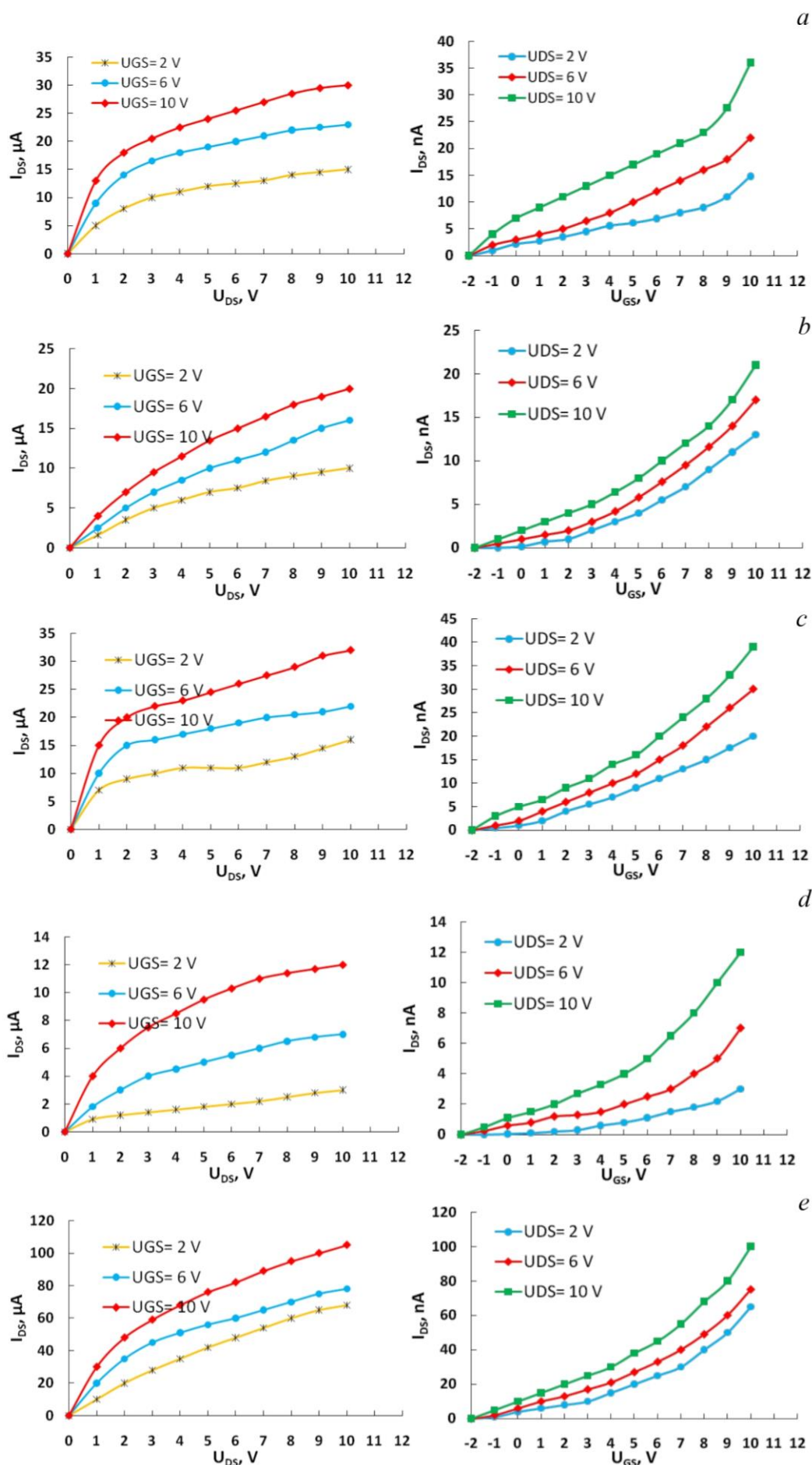
Samples of a new polymer composite material based on a polyelectrolyte complex of chitosan and chitosan succinamide (PEC) doped with various carbon nanomaterials taken in different weight ratios relative to the main polymer matrix were prepared. Electrophysical studies were carried out to measure the effective surface area of sensors and the electron transfer rate. Using the cyclic voltammetry and electrochemical impedance spectroscopy methods, it was found that composite sensors had a sufficiently high effective surface area and electron transfer rate, which allows them to be used in the future in the electroanalysis of compounds of various nature. The use of SWCNTs as dopants is especially effective, since the sensors modified by this composites have the largest active surface areas and the lowest charge transfer rate.

Based on the films studied, field-effect transistors were created and their output and transfer characteristics were measured. The mobility of charge carriers was estimated and the following values were obtained:  $\mu(\text{PEC}) = 0.34$   $\text{cm}^2 \cdot \text{V}^{-1} \cdot \text{s}^{-1}$ ;  $\mu(\text{PEC}/\text{GO}) = 0.97$   $\text{cm}^2 \cdot \text{V}^{-1} \cdot \text{s}^{-1}$ ;  $\mu(\text{PEC}/\text{CP}) = 0.96$   $\text{cm}^2 \cdot \text{V}^{-1} \cdot \text{s}^{-1}$ ;  $\mu(\text{PEC}/\text{CB}) = 0.57$   $\text{cm}^2 \cdot \text{V}^{-1} \cdot \text{s}^{-1}$ ;  $\mu(\text{PEC}/\text{SWCNT}) = 1.12$   $\text{cm}^2 \cdot \text{V}^{-1} \cdot \text{s}^{-1}$ . If a combination of both GO and SWCNT is incorporated into the nanocomposite, the mobility of carriers increases sharply and amounts to  $\mu(\text{PEC}/\text{GO} + \text{SWCNT}) = 10.97$   $\text{cm}^2 \cdot \text{V}^{-1} \cdot \text{s}^{-1}$ .

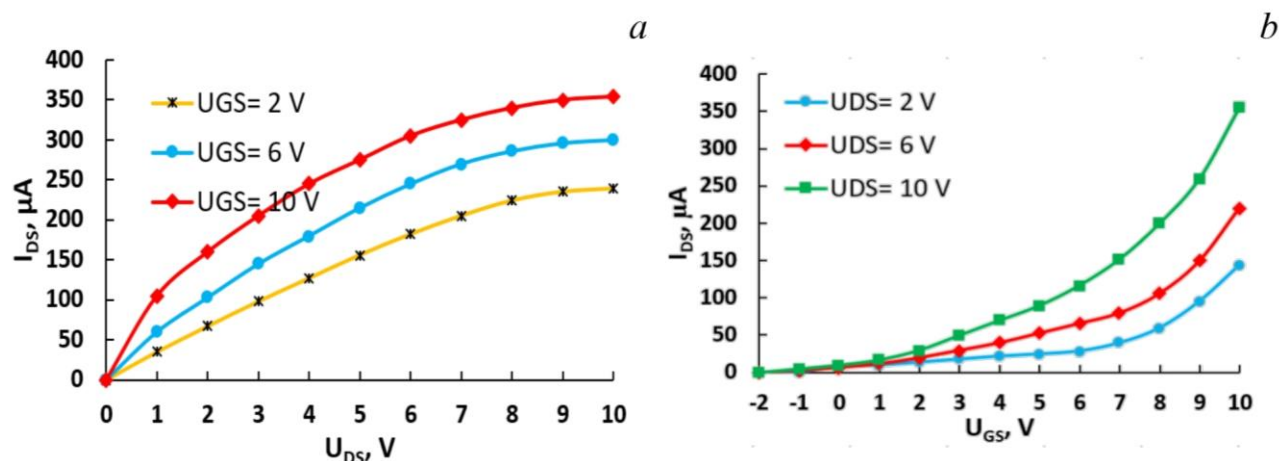


**Figure 8** SEM images taking the chemical composition.





**Figure 9** Output (left) and transfer (right) characteristics of a field-effect transistor with an active layer of PEC (a), PEC-GO (b), PEC-Carbopack (c), PEC-CarboBlackC (d), PEC-SWCNT (e).



**Figure 10** Output (a) and transfer (b) characteristics of a field-effect transistor with an active layer of PEC-SWCNT-GO (synergism effect).

## • Supplementary materials

This manuscript contains supplementary materials, which are available on the corresponding online page.

## • Funding

This work was supported by the Ministry of Science and Higher Education of the Russian Federation (scientific code FZWU-2023-0002) and by the Russian Science Foundation (Grant № 23-73-00119), <https://rscf.ru/project/23-73-00119/>.

## • Acknowledgments

None.

## • Author contributions

Conceptualization: R.Z., R.S.

Data curation: R.Z., R.S.

Formal Analysis: E.B., T.S., A.O.

Funding acquisition: R.S., I.V.

Investigation: Y.T., I.M., A.O., E.B.

Methodology: I.M., Y.T.

Project administration: R.Z., R.S.

Resources: R.S., I.V.

Software: R.S., R.Z., I.V.

Supervision: R.S., R.Z., I.V.

Validation: R.Z., R.S.

Visualization: I.V.

Writing – original draft: R.Z., R.S., Y.T., I.M.

Writing – review & editing: R.Z., R.S., I.V.

## • Conflict of interest

The authors declare no conflict of interest.

## • Additional information

Authors IDs:

Rufina Zilberg, Scopus ID [56572878300](https://orcid.org/0000-0001-9142-1000);

Renat Salikhov, Scopus ID [11738898100](https://orcid.org/0000-0001-9142-1000);

Ilnur Mullagaliev, Scopus ID [57205464144](https://orcid.org/0000-0001-9142-1000);

Yulia Teres, Scopus ID [59012682900](https://orcid.org/0000-0001-9142-1000);

Elena Bulysheva, Scopus ID [57860432900](https://orcid.org/0000-0001-9142-1000);

Timur Salikhov, Scopus ID [55921773000](https://orcid.org/0000-0001-9142-1000);

Ivan Vakulin, Scopus ID [6507180364](https://orcid.org/0000-0001-9142-1000);

Website:

Ufa University of Science and Technology,  
<https://study.uust.ru/>.

## References

- Xu J, Wang S, Wang GJN, Zhu C, Luo S, Jin L, Gu X, Chen S, Feig VR, To JWF, Rondeau-Gagné S, Park J, Schroeder BC, Lu C, Oh JY, Wang Y, Kim YH, Yan H, Sinclair R, Zhou D, Xue G, Murmann B, Linder C, Cai W, Tok JBH, Chung JW, Bao Z. Highly stretchable polymer semiconductor films through the nanoconfinement effect. *Sci.* 2017;355(6320):59–64. doi:[10.1126/science.aah4496](https://doi.org/10.1126/science.aah4496)
- Punetha VD, Rana S, Yoo HJ, Chaurasia A, Mcleskey JT, Ramasamy MS, Sahoo NK, Cho JW. Functionalization of carbon nanomaterials for advanced polymer nanocomposites: a comparison study between CNT and grapheme. *Prog Polym Sci.* 2017;67(14):1–47. doi:[10.1016/j.progpolymsci.2016.12.010](https://doi.org/10.1016/j.progpolymsci.2016.12.010)
- Taherpour AA, Mousavi F. Carbon nanomaterials for electroanalysis in pharmaceutical applications. *Fullerens Graph Nanotubes.* 2018;169–225. doi:[10.1016/B978-0-12-813691-1.00006-3](https://doi.org/10.1016/B978-0-12-813691-1.00006-3)
- Thompson BC, Fre´chet JM. Polymer–fullerene composite solar cells. *Angew Chem Int Ed.* 2008;47(1):58–77. doi:[10.1002/anie.200702506](https://doi.org/10.1002/anie.200702506)
- Liu J, Rinzler AG, Dai H, Hafner JH, Bradley RK, Boul P, Lu A, Iverson TW, Shelimov K, Huffman CB, Rodriguez-Macias FJ, Shon YS, Lee TR, Colbert DT, Smalley RE. Fullerene Pipes. *Sci.* 1998;280(5367):1253–1256. doi:[10.1126/science.280.5367.1253](https://doi.org/10.1126/science.280.5367.1253)
- Jiao LY, Zhang L, Wang XR, Diankov G, Dai HJ. Narrow graphene nanoribbons from carbon nanotubes. *Nature.* 2009;458(7240):877–880. doi:[10.1038/nature07919](https://doi.org/10.1038/nature07919)
- Saito R, Dresselhaus MS, Dresselhaus G. *Physical properties of carbon nanotubes.* Imperial College Press: Singapore; 1998. 3–26.
- Dekker C, Tans SJ, Verschueren ARM. Room-temperature transistor based on a single carbon nanotube. *Nature.* 1998;393(6680):49–52. doi:[10.1038/29954](https://doi.org/10.1038/29954)
- De Heer WA, Chatelain A, Ugarte D. A carbon nanotube field-emission electron source. *Sci.* 1995;270(5239):1179–1180. doi:[10.1126/science.270.5239.1179](https://doi.org/10.1126/science.270.5239.1179)

10. Thostenson ET, Ren Z, Chou TW. Advances in the science technology of carbon nanotubes and their composites: a review. *Compos Sci Technol*. 2001;61(13):1899–1912. doi:[10.1016/S0266-3538\(01\)00094-X](https://doi.org/10.1016/S0266-3538(01)00094-X)
11. Eletsii AV, Knizhnik AA, Potapkin BV, Kenny JM. Electrical characteristics of carbon nanotube-doped composites. *Phy-Usp*. 2015;58(3):209–251. doi:[10.3367/UFNe.0185.201503a.0225](https://doi.org/10.3367/UFNe.0185.201503a.0225)
12. Brady GJ, Way A, Safron NS, Evensen H, Gopalan P, Arnold M. Quasi-ballistic carbon nanotube array transistors with current density exceeding Si and GaAs. *Sci Adv*. 2016;2(9):e1601240. doi:[10.1126/sciadv.1601240](https://doi.org/10.1126/sciadv.1601240)
13. Ziyatdinova GK, Budnikov HC. Carbon nanomaterials and surfactants as electrode surface modifiers in organic electroanalysis. *Nanoanal.: Nanoobjects. Nanotech Anal Chem*. 2018;223–253. doi:[10.1515/9783110542011-007](https://doi.org/10.1515/9783110542011-007)
14. Kour R, Arya S, Young S-J, Gupta V, Bandhoria P, Khosla A. Recent advances in carbon nanomaterials as electrochemical biosensors. *J Electrochem Soc*. 2020;167(3):037555. doi:[10.1149/1945-7111/ab6bc4](https://doi.org/10.1149/1945-7111/ab6bc4)
15. Ziyatdinova GK, Budnikov HC, Zhupanova AS. Electrochemical sensors for the simultaneous detection of phenolic antioxidants. *J Anal Chem*. 2022;77(2):155–172. doi:[10.1134/S1061934822020125](https://doi.org/10.1134/S1061934822020125)
16. Yiğit A, Alpar N, Yardım Y, Çelebi M, Şentürk Z. A graphene-based electrochemical sensor for the individual, selective and simultaneous determination of total chlorogenic acids, vanillin and caffeine in food and beverage samples. *Electroanal*. 2018;30(9):2011–2020. doi:[10.1002/elan.201800229](https://doi.org/10.1002/elan.201800229)
17. Parshina AV, Safronova EY, Habtemariam GZ, Ryzhikh EI, Prikhno IA, Bobreshova OV, Yaroslavtsev AB. Potentiometric sensors based on mf-4sc membranes and carbon nanotubes for the determination of nicotinic acid in aqueous solutions and pharmaceuticals. *Membr Membr Technol*. 2020(4):256–264. doi:[10.1134/S2517751620040083](https://doi.org/10.1134/S2517751620040083)
18. Murtada K, Moreno V. Nanomaterials-based electrochemical sensors for the detection of aroma compounds - towards analytical approach. *J Electroanal Chem*. 2020;861:113988. doi:[10.1016/j.jelechem.2020.113988](https://doi.org/10.1016/j.jelechem.2020.113988)
19. Yola ML. Development of novel nanocomposites based on graphene/graphene oxide and electrochemical sensor applications. *Curr Anal Chem*. 2019;15(2):159–165. doi:[10.2174/1573411014666180320111246](https://doi.org/10.2174/1573411014666180320111246)
20. Krishnan SK, Singh E, Singh P, Meyyappan M, Nalwa HS. A review on graphene-based nanocomposites for electrochemical and fluorescent biosensors. *RSC Adv*. 2019;9(16):8778–8881. doi:[10.1039/C8RA09577](https://doi.org/10.1039/C8RA09577)
21. Kuzikov AV, Bulko TV, Koroleva PI, Masamrekh RA, Babkina SS, Gilep AA, Shumyantseva VV. Cytochrome P450 3A4 as a drug metabolizing enzyme: the role of sensor system modifications in electrocatalysis and electroanalysis. *Biochem Suppl Ser B Biomed Chem*. 2020(4)(3):252–259. doi:[10.1134/S1990750820030075](https://doi.org/10.1134/S1990750820030075)
22. Zilberg R, Teres Yu, Agliulin M, Vakulin I, Bulysheva E, Sycheva M, Maistrenko V. Chiral voltammetric sensor on the basis of nanosized MFI zeolite for recognition and determination of tryptophan enantiomers. *Electroanal*. 2024;36(5):e202300375. doi:[10.1002/elan.202300375](https://doi.org/10.1002/elan.202300375)
23. Zilberg RA, Teres JB, Bulysheva EO, Vakulin IV, Mukhametdinov GR, Khromova OV, Panova MV, Medvedev MG, Maleev VI, Larionov VA. Chiral octahedral cobalt(III) complex immobilized on Carbolblack C as a novel robust and readily available enantioselective voltammetric sensor for the recognition of tryptophan enantiomers in real samples. *Electrochim Acta*. 2024;492:144334. doi:[10.1016/j.electacta.2024.144334](https://doi.org/10.1016/j.electacta.2024.144334)
24. Vakulin IV, Zilberg RA, Galimov II, Sycheva MA. Homochiral zeolites as chiral modifier for voltammetry sensors with high enantioselectivity. *Chirality*. 2023;36(2):e23635. doi:[10.1002/chir.23635](https://doi.org/10.1002/chir.23635)
25. Zilberg RA, Maistrenko VN, TeresYuB, Vakulin IV, Bulysheva EO, Seluyanova AA. A Voltammetric Sensor Based on Aluminophosphate Zeolite and a Composite of Betulinic Acid with Chitosan Polyelectrolyte Complex for the Identification and Determination of Naproxen Enantiomers. *J Anal Chem*. 2023;78(7):933–944. doi:[10.1134/S1061934823070158](https://doi.org/10.1134/S1061934823070158)
26. Salikhov RB, Zilberg RA, Mullagaliev IN, Salikhov TR, Teres YB. Nanocomposite thin film structures based on polyarylenephthalide with SWCNT and graphene oxide fillers. *Mendeleev Commun*. 2022;32(4):520–522. doi:[10.1016/j.mencom.2022.07.029](https://doi.org/10.1016/j.mencom.2022.07.029)
27. Tuktarov AR, Salikhov RB, Khuzin AA, Popod'ko NR, Sa-fargalin IN, Mullagaliev IN, Dzhemilev UM. Photocontrolled organic field effect transistors based on the fullerene C60 and spiropyran hybrid molecule. *RSC Adv*. 2019;9:7505–7508. doi:[10.1039/C9RA00939F](https://doi.org/10.1039/C9RA00939F)
28. Salikhov RB, Biglova YN, Yumaguzin YM, Salikhov TR, Miftakhov MS, Mustafin AG. Solar-energy photoconverters based on thin films of organic materials. *Tech Phys Lett*. 2013;39(10):854–857. doi:[10.1134/S1063785013100106](https://doi.org/10.1134/S1063785013100106)
29. Tuktarov AR, Salikhov RB, Khuzin AA, Safargalin IN, Mullagaliev IN, Venidiktova OV, Valova TM, Barachevsky VA, Dzhemilev UM. Optically controlled field effect transistors based on photochromic spiropyran and fullerene C60 films. *Mendeleev Commun*. 2019;29(2):160–162. doi:[10.1016/j.mencom.2019.03.014](https://doi.org/10.1016/j.mencom.2019.03.014)
30. Ramadhan LOAN, Radiman CL, Suendo V, Wahyuningrum D, Valiyaveettil S. Synthesis and Characterization of Polyelectrolyte Complex N-Succinylchitosan-chitosan for Proton Exchange Membranes. *Procedia Chem*. 2012;4:114–122. doi:[10.1016/j.proche.2012.06.017](https://doi.org/10.1016/j.proche.2012.06.017)
31. Kolesov SV, Gurina MS, Mudarisova RK. Specific features of the formation of aqueous nanodispersions of interpolyelectrolyte complexes based of chitosan and chitosan succinimide. *Russ J Gen Chem*. 2018;88(8):1694–1698. doi:[10.1134/S1070363218080224](https://doi.org/10.1134/S1070363218080224)
32. Kolesov SV, Gurina MS, Mudarisova RK. On the stability of aqueous nanodispersions of polyelectrolyte complexes based on chitosan and N-succinyl-chitosan. *Polym Sci Ser A*. 2019;61(3):253–259. doi:[10.1134/S0965545X19030076](https://doi.org/10.1134/S0965545X19030076)
33. Bazunova MV, Mustakimov RA, Bakirova ER. Conditions of formation of stable polyelectrolyte complexes based on N-succinyl chitosan and poly-N,N-diallyl-N,N-dimethylammonium chloride. *Russ J Appl Chem*. 2022;95(1):46–52. doi:[10.1134/S1070427222010062](https://doi.org/10.1134/S1070427222010062)
34. Barck K, Butler MF. Comparison of morphology and properties of polyelectrolyte complex particles formed from chitosan and polyanionic biopolymers. *J Appl Polym Sci*. 2005;98(4):1581–1593. doi:[10.1002/ap.22177](https://doi.org/10.1002/ap.22177)
35. Boddohi S, Moore N, Johnson PA, Kipper MJ. Polysaccharide-based polyelectrolyte complex nanoparticles from chitosan, heparin, and hyaluronan. *Biomacromolec*. 2009;10(6):1402–1409. doi:[10.1021/bm801513e](https://doi.org/10.1021/bm801513e)
36. Shu XZ, Zhu KJ. Chitosan/gelatin microspheres prepared by modified emulsification and ionotropic gelation. *J Microencapsul*. 2001;18(2):237–245. doi:[10.1080/02652040010000415](https://doi.org/10.1080/02652040010000415)
37. Bernkop-Schnurch A, Dunnhaupt S. Chitosan-based drug delivery systems. *Eur J Pharm Biopharm*. 2012;81(3):463–469. doi:[10.1016/j.ejpb.2012.04.007](https://doi.org/10.1016/j.ejpb.2012.04.007)
38. Gurina MS, Vil'danova RR, Badykova LA, Vlasova NM, Kolesov SV. Microparticles based on chitosan-hyaluronic acid interpolyelectrolyte complex, which provide stability of aqueous dispersions. *Russ J Appl Chem*. 2017;90(2):219–224. doi:[10.1134/S1070427217020100](https://doi.org/10.1134/S1070427217020100)
39. Guo R, Chen L, Cai S, Liu Z, Zhu Y, Xue W, Zhang Y. Novel alginate coated hydrophobically modified chitosan polyelectrolyte complex for the delivery of BSA. *J Mater Sci Mater Med*. 2013;24(9):2093–2100. doi:[10.1007/s10856-013-4977-3](https://doi.org/10.1007/s10856-013-4977-3)
40. Wu D, Zhu L, Li Y, Zhang X, Xu S, Yang G, Delair T. Chitosan-based colloidal polyelectrolyte complexes for drug delivery: a review. *Carbohydr Polym*. 2020;238:116126. doi:[10.1016/j.carbpol.2020.116126](https://doi.org/10.1016/j.carbpol.2020.116126)
41. Zil'berg RA, Zagitova LR, Vakulin IV, Yarkaeva YA, Teres YB, Berestova TV. Enantioselective voltammetric sensors based



- on amino acid complexes of Cu(II), Co(III), and Zn(II). *J Anal Chem.* 2021;76(12):1438–1448. doi:[10.1134/S1061934821120145](https://doi.org/10.1134/S1061934821120145)
42. Zilberg RA, Vakulin IV, Teres YB, Galimov II, Maistrenko VN. Rational design of highly enantioselective composite voltammetric sensors using a computationally predicted chiral modifier. *Chirality.* 2022;34(11):1472–14788. doi:[10.1002/chir.23502](https://doi.org/10.1002/chir.23502)
43. Zilberg RA, Maistrenko VN, Kabirova LR, Dubrovsky DI. Selective voltammetric sensors based on composites of chitosan polyelectrolyte complexes with cyclodextrins for the recognition and determination of atenolol enantiomers. *Anal Methods.* 2018;10(16):1886–1894. doi:[10.1039/C8AY00403J](https://doi.org/10.1039/C8AY00403J)
44. Dos Santos M, Wrobel E, dos Santos V, Quinaia SP, Fujiwara ST, Garcia JR, Pessoa CA, Scheffer EWO, Wohnrath K. Development of an electrochemical sensor based on LbL films of Pt nanoparticles and humic acid. *J Electrochem Soc.* 2016;163(9):B499–B506. doi:[10.1149/2.1001609jes](https://doi.org/10.1149/2.1001609jes)
45. Zanardi C, Terzi F, Zanfognini B, Pigani L, Seeber R, Lukkari J, Ääritalo T. Effective catalytic electrode system based on polyviologen and Au nanoparticles multilayer. *Sens Act B Chem.* 2010;144(1):92–98. doi:[10.1016/j.snb.2009.10.041](https://doi.org/10.1016/j.snb.2009.10.041)
46. Mathi S, Gupta P, Kumar R, Nagarale R, Sharma A. Ferrocenium ion confinement in polyelectrolyte for electrochemical nitric oxide sensor. *Chem Select.* 2019;4(13):3833–3840. doi:[10.1002/slct.20180367](https://doi.org/10.1002/slct.20180367)
47. Škugor Rončević I, Krivić D, Buljac M, Vladislavić N, Buzuk M. Polyelectrolytes assembly: a powerful tool for electrochemical sensing application. *Sensors.* 2020;20(11):3211. doi:[10.3390/s20113211](https://doi.org/10.3390/s20113211)
48. Priftis D. Polyelectrolyte-graphene nanocomposites for biosensing application. *Curr Org Chem.* 2015;19:1819–1827. doi:[10.2174/1385272819666150526005557](https://doi.org/10.2174/1385272819666150526005557)
49. Bard AJ, Faulkner LR. *Electrochemical Methods. Fundamentals and Application.* 2nd edn. John Wiley and Sons: New York; 2004. 850 p.
50. Lasia A. *Electrochemical Impedance Spectroscopy and its Applications.* Springer: NewYork.; 2014; 1–21.
51. Hallani RK, Paulsen BD, Petty AJ, Sheelamanthula R, Moser M, Thorley KJ, Sohn W, Rashid RB, Savva A, Moro S, Parker JP, Drury O, Alsufyani M, Neophytou M, Kosco J, Inal S, Costantini G, Rivnay J, McCulloch I. Regiochemistry-driven organic electrochemical transistor performance enhancement in ethylene glycol-functionalized polythiophenes. *J Am Chem Soc.* 2021;143(29):11007–11018. doi:[10.1021/jacs.1c03516](https://doi.org/10.1021/jacs.1c03516)
52. Jia H, Huang Z, Li P, Zhang S, Wang Y, Wang J-Y, Gu X, Lei T. Engineering donor-acceptor conjugated polymers for high-performance and fast-response organic electrochemical transistors. *J Mater Chem C.* 2021;9(14):4927–4934. doi:[10.1039/D1TC00440A](https://doi.org/10.1039/D1TC00440A)
53. Moser M, Savva A, Thorley K, Paulsen BD, Hidalgo TC, Ohayon D, Chen H, Giovannitti A, Marks A, Gasparini N, Wadsworth A, Rivnay J, Inal S, McCulloch I. Polaron delocalization in donor-acceptor polymers and its impact on organic electrochemical transistor performance. *Angew Chem Int Ed.* 2021;60:7777–7785. doi:[10.1002/anie.202014078](https://doi.org/10.1002/anie.202014078)
54. Inal S, Malliaras GG, Rivnay J. Benchmarking organic mixed conductors for transistors. *Nat Commun.* 2017;8(1):1767. doi:[10.1038/s41467-017-01812-w](https://doi.org/10.1038/s41467-017-01812-w)
55. Luo X, Shen H, Perera K, Tran DT, Boudouris BW, Mei J. Designing donor-acceptor copolymers for stable and high-performance organic electrochemical transistors. *ACS Macro Lett.* 2021;10(8):1061–1067. doi:[10.1021/acsmacrolett.1c00328](https://doi.org/10.1021/acsmacrolett.1c00328)
56. Lan L, Chen J, Wang Y, Li P, Yu Y, Zhu G, Li Z, Lei T, Yue W, McCulloch I. Facilely accessible porous conjugated polymers toward high-performance and flexible organic electrochemical transistors. *Chem Mater.* 2022;34(4):1666–1676. doi:[10.1021/acs.chemmater.1c03797](https://doi.org/10.1021/acs.chemmater.1c03797)
57. Budzalek K, Ding H, Janasz L, Wypych-Puszkarcz A, Cetinkaya O, Pietrasik J, Kozanecki M, Ulanski J, Matyjaszewski K. Star polymer-TiO<sub>2</sub> nanohybrids to effectively modify the surface of PMMA dielectric layers for solution processable OFETs. *J Mater Chem C.* 2020;9:1269–1278. doi:[10.1039/D0TC03137B](https://doi.org/10.1039/D0TC03137B)
58. Han S-T, Zhou Y, Yang Q-D, Lee C-S, Roy VAL. Poly(3-hexylthiophene)/gold nanoparticle hybrid system with an enhanced photoresponse for light-controlled electronic devices. *Part Part Syst Charact.* 2013;30(7):599–605. doi:[10.1002/ppsc.201300005](https://doi.org/10.1002/ppsc.201300005)
59. Kim Y, Kwon YJ, Ryu S, Lee CJ, Lee JU. Preparation of nanocomposite-based high performance organic field effect transistor via solution floating method and mechanical property evaluation. *Polymers.* 2020;12(5):1046. doi:[10.3390/polym12051046](https://doi.org/10.3390/polym12051046)
60. Hong K, Yang C, Kim SH, Jang J, Nam S, Park CE. photopatternable source/drain electrodes using multiwalled carbon nanotube/polymer nanocomposites for organic field-effect transistors. *ACS Appl Mater Interfaces.* 2009;1(10):2332–2337. doi:[10.1021/am900483v](https://doi.org/10.1021/am900483v)